Predicting Cancer Outcome with Multispectral Tumor Tissue Images

Jin Qu

A thesis

Submitted in partial fulfillment of the

requirements for the degree of

Master of Science

University of Washington

2017

Committee:

Peter Myler

Ilya Shmulevich

Program Authorized to Offer Degree:

Biomedical and Health Informatics

University of Washington

Abstract

Predicting Cancer Outcome with Multispectral Tumor Tissue Images

Jin Qu

Chair of the Supervisory Committee:

Peter Myler, PhD, Professor

Biomedical and Health Informatics

Tumor tissue slides have been used by clinicians to assess cancer patient's condition and indicate prognosis. Several recent studies have suggested that distribution of important immunological markers on tumor tissue slides might help predict survival outcome [1] [2] [3] [4]. These studies rely upon non-parametric Kaplan-Meier survival analysis with Log-rank test to extract statistical insights, which, however, has several disadvantages such as prediction ambiguity and inability to directly model continuous variables.

In this study, we engineered 676 features encoding cellular distribution information from multi-spectral tumor tissue images collected from 118 HPV-negative oral squamous cell cancer patients. We leveraged statistical methods and predictive models to explore the predictive power

of these features. We identified 18 features as potential survival predictors through Kolmogorov-Smirnov test. Our best model, random forest model, has achieved 58.54% prediction accuracy rate on independent validation dataset. Although the model does not suggest strong predictive power of selected features, evaluation on large scale training data is still needed to further tune model parameters and generate more concrete results.

TABLE OF CONTENTS

ACKNOWLEDGEMENTS

The author would like to express his heartfelt gratitude to the member of his committee, Dr. Ilya Shmulevich and Dr. Peter Myler for their invaluable advice and guidance. He would also like to thank Fred Lu for his previous work on generating features, Dr. Vesteinn Thorsson and Dr. Theo Knijnenburg for their insights and willingness to listen to his thoughts on this project at various and sundry times.

Chapter 1. INTRODUCTION

Recent advancement in Machine Learning and Artificial Intelligence (AI) has shown great promise in various fields in healthcare and life sciences such as drug discovery, automated disease diagnosis and biomedical imaging processing [5]. In this study, we have leveraged various statistical and machine learning methods to explore the predictive power of multi-spectral tumor tissue images from patients with human papillomavirus (HPV)-negative oral squamous cell carcinoma (OSCC).

According to the most recent data from the American Cancer Society (ACS), head and neck cancers account for about 4% of all cancers in the United States (U.S) [6]. Over 90% of head and neck tumors are squamous carcinomas [7]. Traditionally, healthcare providers and researchers have relied upon the standard staging system established by the American Joint Committee on Cancer–International Union Against Cancer -- TNM (tumor size, spread to lymph nodes and metastasis) system [8] to indicate cancer prognosis and help plan treatment strategies. Several recent studies, however, have suggested the ineffectiveness of this system and proposed to leverage important immunological markers such as immune cell location patterns to provide more accurate prediction for prognosis and indicate response to therapy [9] [10] [11]. For example, increased cytotoxic CD8+ T cell infiltration within the tumor region has been proved to be positively correlated with prolonged survival in various cancer types [2] [3] [4]. In contrast, increased presence of intratumoral FOXP3+ T regulatory cells has been linked to poor clinical outcome in various cancers [10][12][13][14]. However, there are few studies on HPV-negative OSCC.

Multiple research projects have used statistical methods such as Kaplan-Meier survival analysis to study immunological features. For example, Eerola and colleagues have used Kaplan-Meier survival analysis and Log-rank test to find out that high number of intratumoral T cells and CD8+ T cells indicates favorable survival outcome compared with patient groups with either low number of intratumoral T cells or CD8+ T cells ($P = 0.007 / 0.02$) [2] in small cell lung carcinoma (SCLC) patients.

Kaplan-Meier survival analysis with Log-rank test has been widely used in the biomedical field to provide statistical insights on the differences between groups [15]. However, this method suffers from several disadvantages:

1) Kaplan-Meier survival analysis requires input data to be categorical. If the input dataset is numerical, people have to group the whole dataset into different categories based on empirical or other subjective evidence, which is not always readily available nor accurate.
2) Kaplan-Meier survival analysis produces qualitative results instead of quantitative survival estimation. For example, in the aforementioned study by Eerola, the results generated from Kaplan-Meier survival analysis suggest that patients with higher number of intratumoral T cells and CD8+ T cells are associated with better survival outcome. However, this analysis is unable to specify exact survival time and therefore introduces ambiguity.
3) Kaplan-Meier survival analysis focuses on survival outcome at the group level instead of at individual level, which results in the situation that an observation found at the group level does not always apply to each patient. For example, although the Kaplan-Meier

curve is able to present statistically significant differentiation of survival probability in two patient groups, the survival chance of an individual patient requires further analysis.

4) It is difficult to study the interplay of different variables using Kaplan-Meier survival analysis. For example, in a clinical trial, if a researcher wants to study the interaction of a certain drug with patients' demographics information such as gender, age, etc., the researcher has to assign patients into different groups accordingly. The assignment operation is not only laborious, but will also result in multiple groups and thus fewer observations in each group.

Therefore, it is necessary to leverage other modeling and analytical methods to overcome these shortcomings. Machine learning methods, particularly classification methods, can be used to take clinical data as input and output survival probability at a specific time, which generates a more quantitative survival time prediction than the Kaplan-Meier model does. Machine learning methods can also automatically model linear or nonlinear relationship among different variables within the dataset and enjoy great flexibility of model different types of variables.

Multispectral tumor tissue images in this study were obtained through staining tumor tissue slides with multiple biochemical products and analyzed via the PerkinElmer Vectra imaging platform (http://www.perkinelmer.com/) for further analysis. Details about staining and analysis were described by our collaborator, Dr. Zipei Feng, in his publication "Multiparametric Analysis of Tumor Immune Environment" [16].

Chapter 2. DATA

In total, 157 multi-spectral tumor tissue images from 118 patients with HPV-negative OSCC were included in this study. Figure 1 shows the Kaplan-Meier survival curve of the population in this study. More Detailed information about the 118 patients can be found in Appendix 1.

Tumor tissue materials were prepared and handled by our collaborators at the Earle A. Chiles Research Institute in Portland, Oregon, USA [20]. Raw images were processed by them with PerkinElmer inForm (http://www.perkinelmer.com/) software to extract cell location information (See details in Appendix 1).

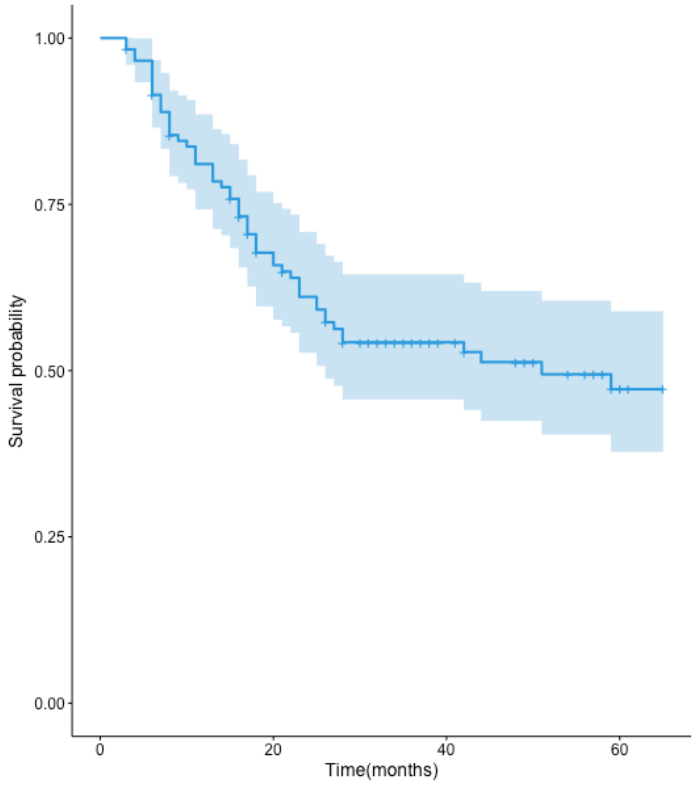

Figure 1. Kaplan-Meier Survival Curve

Item	Proportion	Item	Proportion
Male	75.4%	Female	24.6%
Death (at last follow-up)	53.3%	Alive(at last follow-up)	46.6%
Stage I	14.4%	Stage II	19.5%
Stage III	11.9%	Stage IV	54.2%

Table 1. Summary Statistics of Participants

	Age (years)	Survival Time (months)
Minimum	25	3
1st Quantile	51	15
Median	58	26
Mean	58.68	30.99
3rd Quantile	68	48.75
Maximum value	83	65
Number of missing values	11	0

Table 2. Summary Statistics of Participants. Table 1 together with Table 2 provides an overview of the patient cohort in this study.

We programmed MATLAB (https://www.mathworks.com/) code to generate features that describe cellular distribution based upon cell location dataset. Figure 2 illustrates the workflow

of how features were calculated. In the end, we introduced 676 features. Appendix 2 contains a list of all the names of features included in this study.

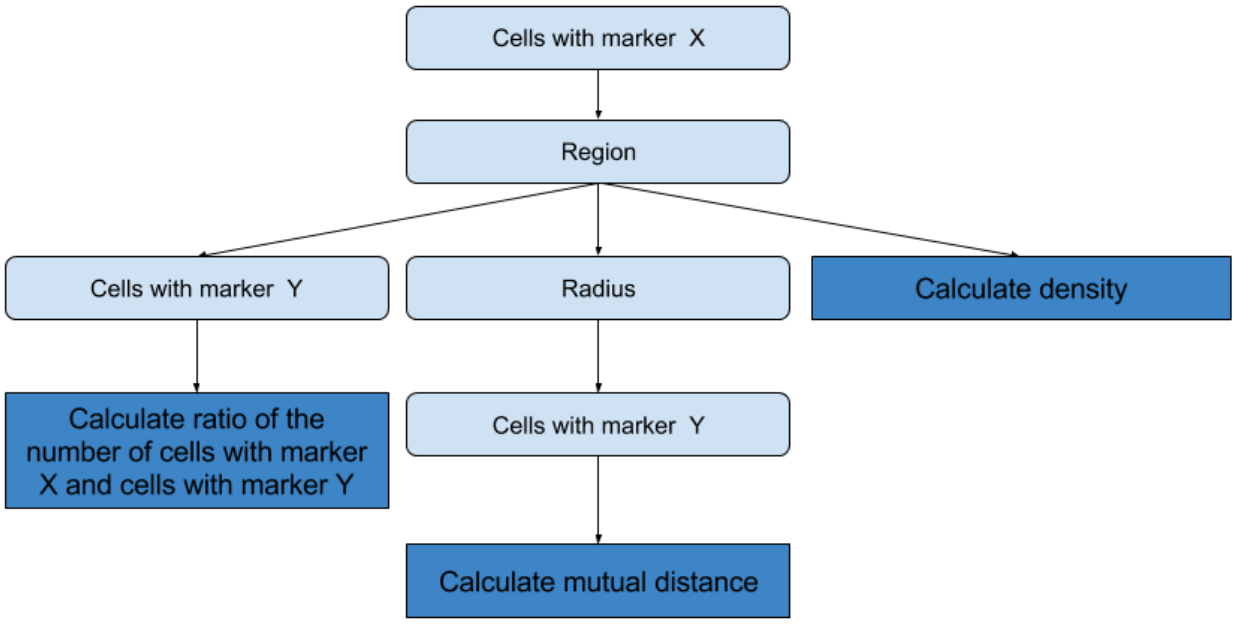

Figure 2. Workflow of Feature Generation. In this figure, marker X or Y can be any one of CD-4, CD-8, PD-L1, CD-163, FOXP3 or DAPI. Regions can be tumor region, stroma region or the whole image region. For example, the feature named as 'mean_cd8_foxp3_100_t' means the averaged proportion of FOXP3+ cells within 100 micron of each CD-8+ cell.

1. Missing Values and Infinite Values

Missing values (denoted as 'NA' in R) and infinite values (denoted as 'Inf') were generated during the feature calculation process. For example, feature 'mean_cd4_r_foxp3_tumor' means the ratio of the number of $CD4^+$ cells and the number of $FOXP3^+$ cells in the tumor region. If the

numerator (the number of $CD4^+$ cells) and the denominator (the number of $FOXP3^+$ cells) are both zero, a 'NA' value is introduced. However, if the numerator is a non-zero integer while the denominator is zero, an 'Inf' value will be generated.

We investigated the proportion of missing values and infinite values across the entire feature set. Figure 3 and Figure 4 shows the boxplot of the proportion of missing values and infinite values within each feature. Both missing and infinite values were transformed to be 0 in the analysis to encode that there is no information associated with its corresponding feature.

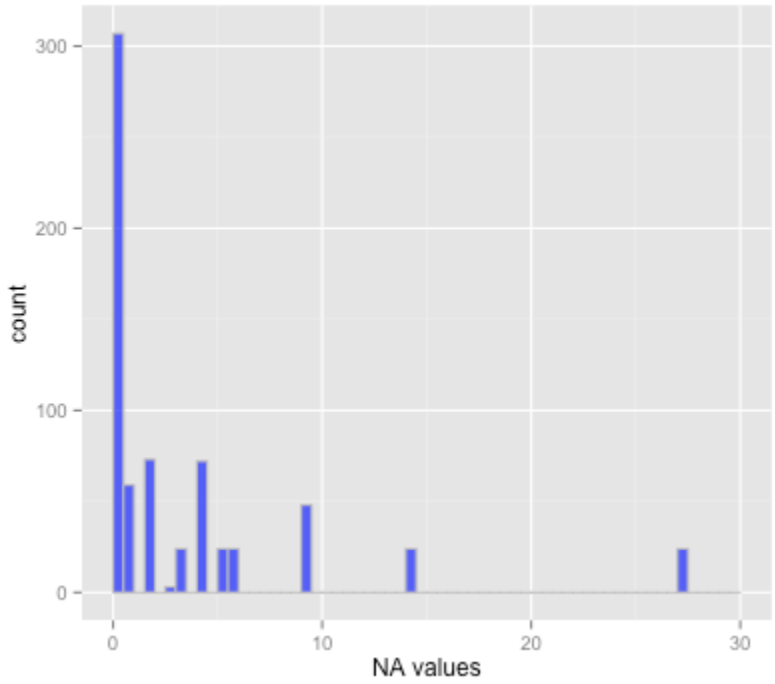

Figure 3. Histogram of proportion of NA values (1%/bin). The highest percentage is 27.12 %, average percentage is 3.34% and median percentage is 0.85%.

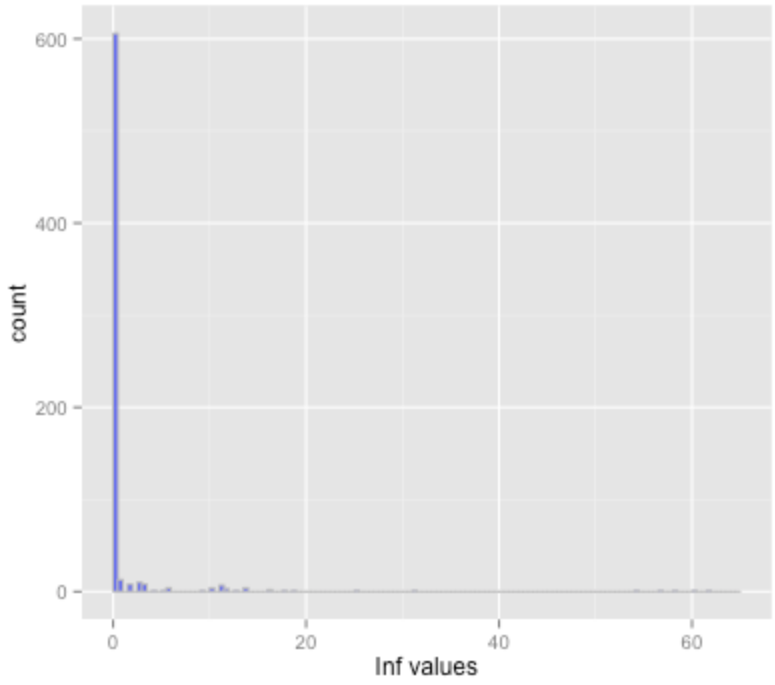

Figure 4. Histogram of proportion of Inf values (1%/bin). The highest percentage is 61.86 %, average percentage is 1.11% and median percentage is 0%.

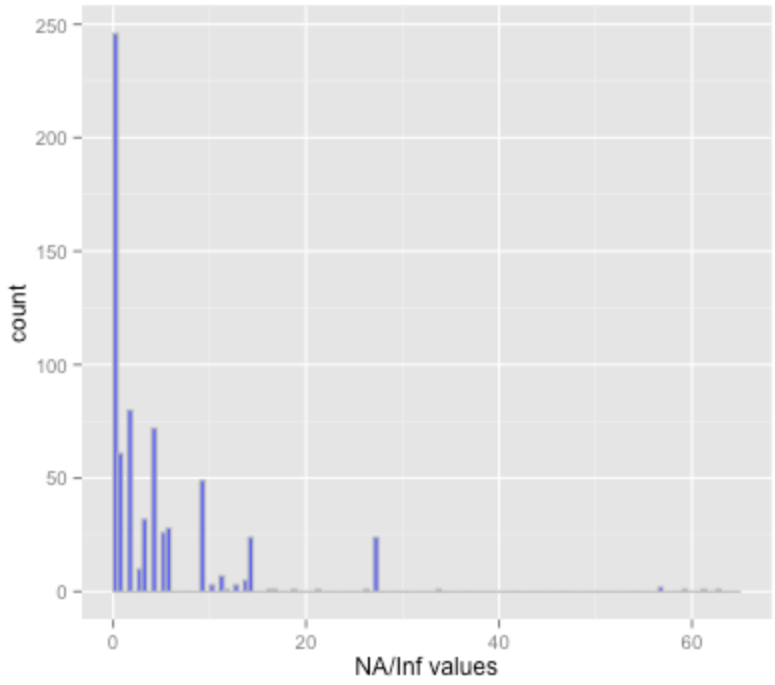

Figure 5. Histogram of proportion of NA or Inf values (1%/bin). The highest percentage is 62.71 %, average percentage is 4.45% and median percentage is 1.70%.

2. Linear Correlation

We used Pearson correlation score to study linear correlation between each feature pair. Figure 5 is a heatmap showing the correlation structure within the feature set.

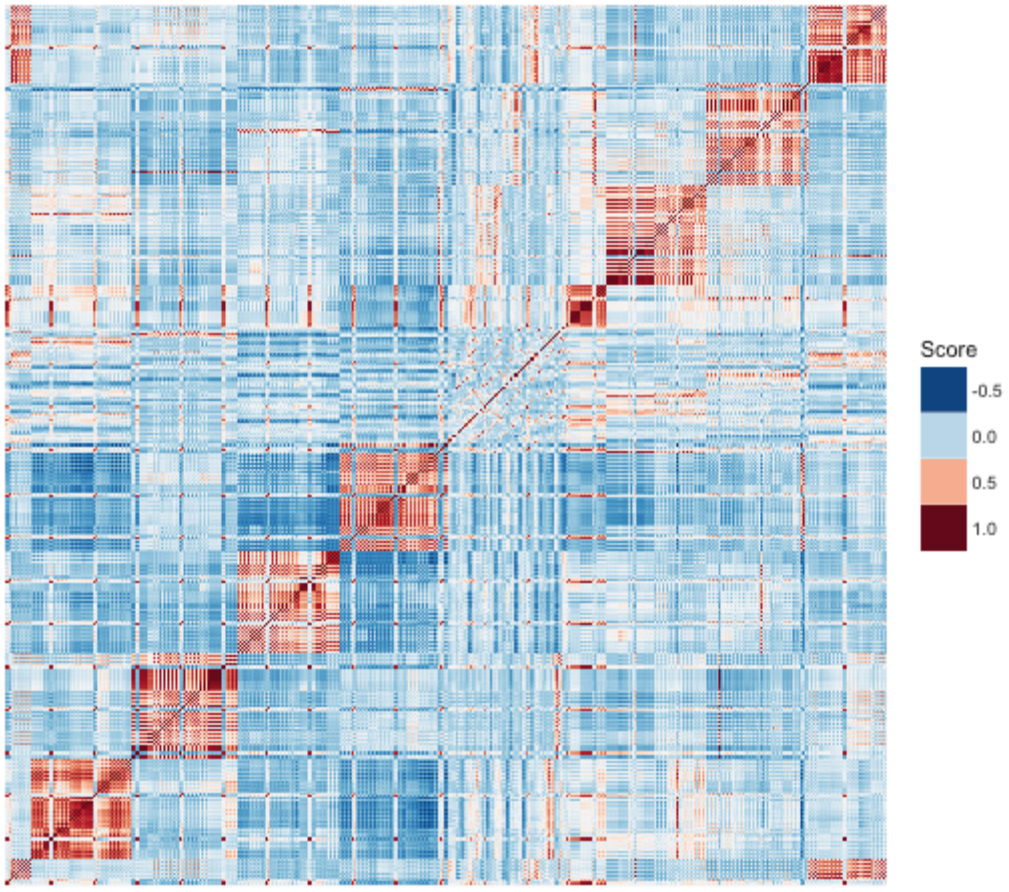

Figure 5. Heatmap of Linearity Across Features. In this figure, blue color indicates negative linear correlation while red color indicates positive linear correlation. This figure shows that correlation structure exists within the feature set.

3. Follow-up Time Distribution

Figure 6 provides an overview of follow-up time. The longest overall follow-up time is 65 months while the shortest is 3 months with the median of 26 months and the mean of 30.99 months.

The number of patients included in this study is 118 in total. 55 out of these patients have been identified as deceased at the last follow-up and 63 were alive at the time of follow-up.

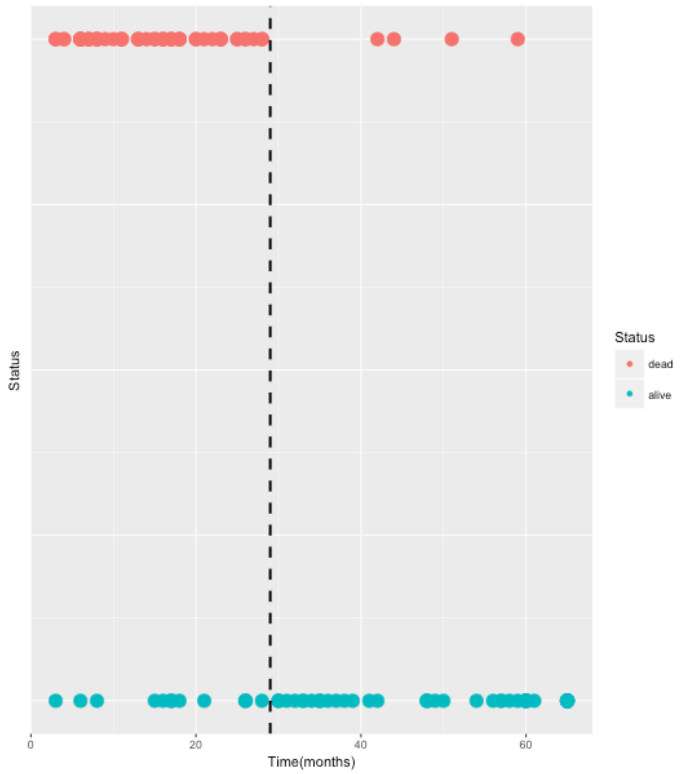

Figure 6. Follow-up Time Distribution. The dashed line denotes the 30th month. The red dots represent patients who died at follow-up during the study. The green dots represent patients who were still alive at the last follow-up.

Chapter 3. MODELING

When using machine learning methods for classification, it is often important to have each class roughly equal-sized because an unbalanced dataset would cause the learning algorithm biased towards the majority class. We noted that at around 30th month of follow-up time, the number of patients whose status was alive almost equals the number of patients who were deceased (50:51). Therefore, we set our prediction goal to be predicting patients' 30th month survival rate. We first tried a simple machine learning method -- Logistic Regression as a baseline model and then used a more complicated model -- Random Forest to predict 30-month survival probability.

Tools

All the analysis and plots were done on an iMac computer (21.5-inch, late 2013) with R programming language (version: 3.2.1, https://cran.r-project.org/) and Rstudio (version: 0.99.447, https://www.rstudio.com/) as an integrated programming environment (IDE).

Kaplan-Meier curve was plotted using the package 'survminer' (version: 0.3.1, https://cran.r-project.org/web/packages/survminer/index.html). Other plots were done using the package 'ggplot2' (version: 1.0.1, https://cran.r-project.org/web/packages/ggplot2/).

Logistic regression modeling was done using R built-in package 'stats' (version: 3.1.3) and the package 'boot' (version: 1.3-15, https://cran.r-project.org/web/packages/boot/) [18] for cross-validation. Random forest modeling was done with the package 'randomForest' (version 4.6-10, https://cran.r-project.org/web/packages/randomForest/) [19] and 'caret' (version 6.0-47, https://cran.r-project.org/web/packages/caret/) for parameter tuning.

Cox proportional hazards model was trained using R built-in package 'survival' (version: 2.38-1, https://cran.r-project.org/web/packages/survival/index.html) [20].

Feature Selection

The whole feature set was split into two groups according to patients' one-year survival status and compared using the two-sided Kolmogorov–Smirnov test (K-S test) [17]. Only features with P-values less than 0.025 (95% confidence level) were included in the following analysis. With K-S test, we reduced 676 features in total to 54 features.

Features were then further reduced by manually selecting one representative feature from each similar feature sub-groups. For example, consider three features: 'mean_cd8_cd8_60', 'mean_cd8_cd8_60_s' and 'mean_cd8_cd8_100'. All of them were calculated based on the averaged mutual distance of CD8+ cells, but within different radii. The feature 'mean_cd8_cd8_60' was calculated within the radius of 60 microns of each CD8 + while 'mean_cd8_cd8_60_s' was calculated likewise but only within the stroma region of the image. Feature 'mean_cd8_cd8_100', on the other hand, was calculated within the radius of 100 microns. Although the scope under which these three features were generated vary, these features often ended up with the same or very similar numeric values. Figure 7 shows the similarity of the distributions of these three features. To reduce this redundancy, we only select the feature with the lowest P-value from these three to represent this feature sub-group. We also went over every single distribution plot within each feature sub-group to confirm if their distribution looks similar. If there was more than one feature having the same lowest P-value, we

selected the feature that has been calculated at the largest scale. For example, if both feature 'mean_cd8_cd8_60_s' and 'mean_cd8_cd8_100' have the same lowest P-value, we only considered 'mean_cd8_cd8_100' because it was calculated within a 100 micron radius of each CD8+ cell while the feature 'mean_cd8_cd8_60_s' was calculated at the scale of 60 microns and within the stroma region.

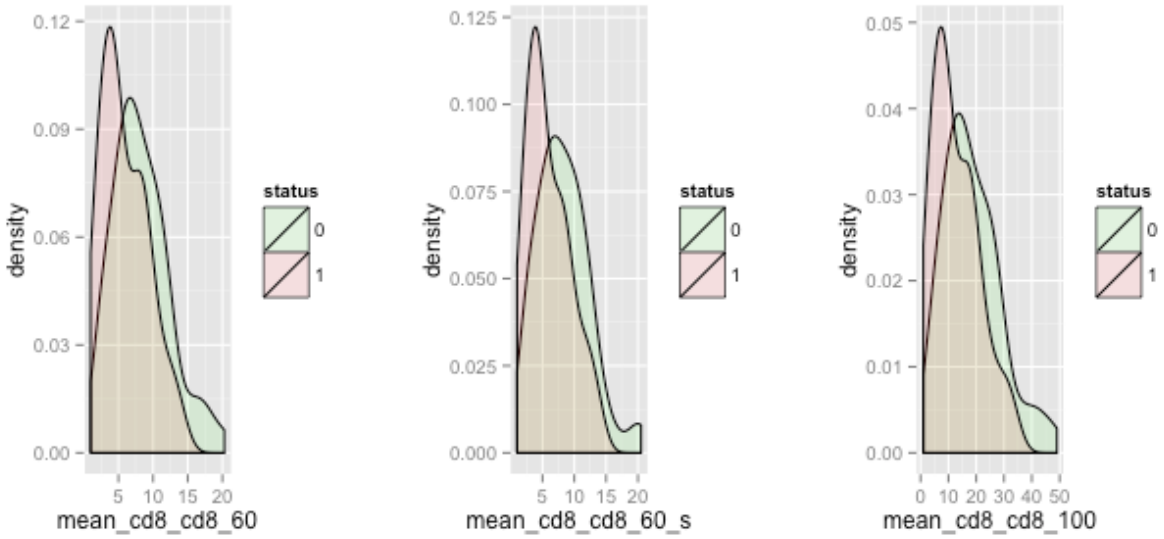

Figure 7. Density Plot of Three Features with Similar Numeric Values. This figure indicates that although feature of 'mean_cd8_cd8_60', 'mean_cd8_cd8_60_s' and 'mean_cd8_cd8_100' were calculated within different radii, they have quite similar numeric values.

After applying the K-S test and further feature reduction, the total feature set was reduced to 18 features. Table 3 lists all these 18 features and their corresponding P-value. Density plots of these features can be seen in Figure 8.

Feature Name	P-value
mean_cd8_stroma	0.017553809
mean_macs_pdl1_30	0.028789376
mean_cd4_cd8_100_s	0.009021174
mean_pdl1mac_other_30_s	0.040316014
mean_foxp3_cd8_100	0.001351267
mean_tumor_other_100_s	0.011544996
mean_macs_tumor_30	0.031185923
mean_other_tumor_30	0.018668997
mean_pdl1mac_cd8_100_s	0.011944919
mean_cd8_r_foxp3_stroma	0.031705197
mean_cd8_r_pdl1mac	0.002411018
mean_cd8_r_other	0.018668997
mean_cd8_r_tumor	0.028460621
mean_cd4_r_pdl1mac	0.032265628
mean_pdl1_cd8_100	0.003814411
mean_other_cd8_100	0.017553809
mean_tumor_cd8_100_s	0.009587529
mean_cd8_cd8_30_s	0.001042085

Table 3. A List of 18 Features Selected by K-S Test (95% significant level) and Further Dimension Reduction.

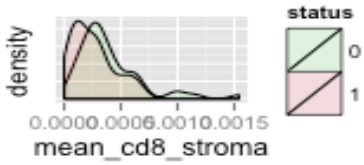
density
0.0000 0.0005 0.0010 0.0015
mean_cd8_stroma
status
0
1

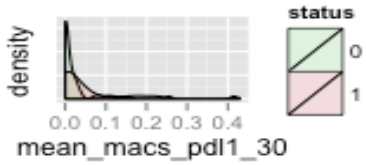
density
0.0 0.1 0.2 0.3 0.4
mean_macs_pdl1_30
status
0
1

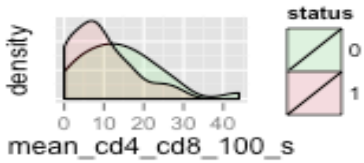
density
0 10 20 30 40
mean_cd4_cd8_100_s
status
0
1

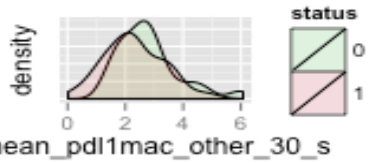
density
0 2 4 6
mean_pdl1mac_other_30_s
status
0
1

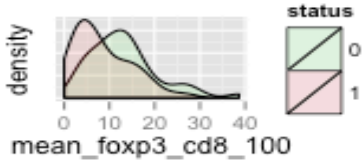
density
0 10 20 30 40
mean_foxp3_cd8_100
status
0
1

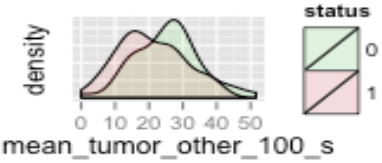
density
0 10 20 30 40 50
mean_tumor_other_100_s
status
0
1

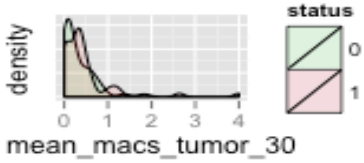
density
0 1 2 3 4
mean_macs_tumor_30
status
0
1

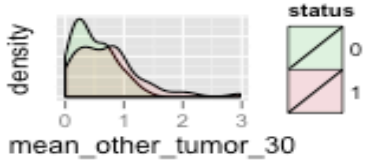
density
0 1 2 3
mean_other_tumor_30
status
0
1

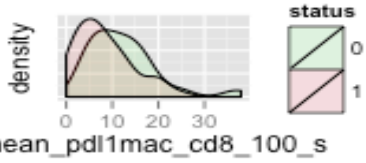
density
0 10 20 30
mean_pdl1mac_cd8_100_s
status
0
1

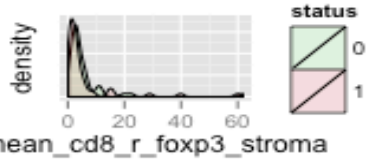
density
0 20 40 60
mean_cd8_r_foxp3_stroma
status
0
1

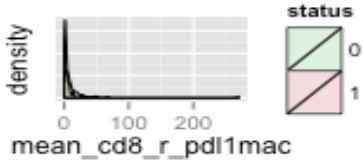
density
0 100 200
mean_cd8_r_pdl1mac
status
0
1

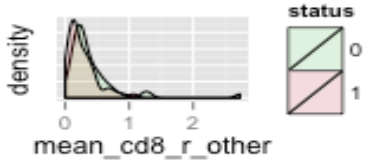
density
0 1 2
mean_cd8_r_other
status
0
1

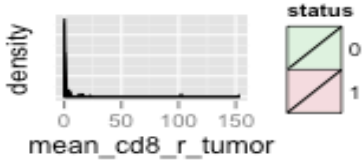
density
0 50 100 150
mean_cd8_r_tumor
status
0
1

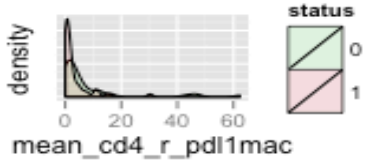
density
0 20 40 60
mean_cd4_r_pdl1mac
status
0
1

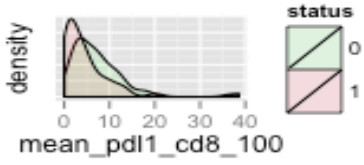
density
0 10 20 30 40
mean_pdl1_cd8_100
status
0
1

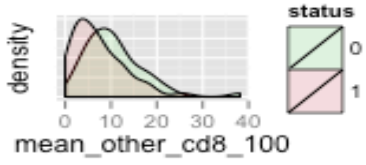
density
0 10 20 30 40
mean_other_cd8_100
status
0
1

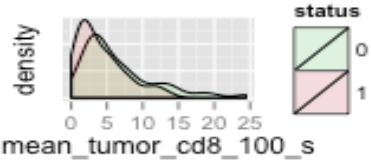
density
0 5 10 15 20 25
mean_tumor_cd8_100_s
status
0
1

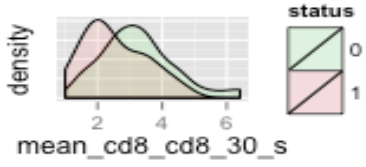
density
2 4 6
mean_cd8_cd8_30_s
status
0
1

Figure 8. Density Plots of 18 Final Feature Set

Data Processing

Patients who were still alive and whose last follow-up ended before the 30th month were excluded from modeling because of uncertainty about final status. In the end, there were 101 observations included in this 30-month survival prediction study in total. The whole dataset was randomly split into training and testing datasets. 60 observations were selected for the training dataset while 41 observations for the testing dataset.

Logistic Regression Model

Logistic Regression model was trained on the training dataset with 5-fold cross-validation to mitigate over-fitting. The trained model was then tested on the independent testing dataset. Results are presented in Chapter 5.

Random Forest Model

Model performance results from the Logistic Regression model suggests that the selected 18 features are not able to provide an accurate prediction of patients' 30-month survival. This indicates that none of the 18 features can be considered as a strong predictor of survival. With this observation taken into consideration, we tried the Random Forest method, which has been designed to combine multiple predictors in an ensembling fashion in order to generate more accurate predictions [21]. We used the R package, 'randomForest-4.6-10' for random forest modeling and 'caret-6.0-47' for parameter tuning.

There are two hyper-parameters in random forest model, ‘mtry’ -- number of variables randomly sampled as candidates at each split, ‘ntree’ -- number of trees to grow [19]. The possible value for ‘mtry’ has been set to be any integer within 1-18 range while ‘ntree’ can be any any integer of the set -- 1, 10, 20, 30, 50, 80, 100, 120, 150, 200. We used grid search method to exhaust all the possible parameter combinations and leveraged train function in ‘caret’ package to automate the process.

With each model evaluated using 5-fold cross validation, we found the model with ‘mtry’ been set to be 1 and ‘ntree’ been set to be 20 enjoys a high accuracy rate (~63.33%) and a low variation during cross validation (~ 0.046 standard deviation).

We then trained our random forest model with ‘mtry’ equals to 1 and ‘ntree’ equals to 20 and evaluated model performance on the testing dataset. The confusion matrix that has been used to assess the model performance on the testing dataset can be found at Table 5.

Cox Proportional Hazards Model

To further investigate other modeling methods and compare the performance of classification model and survival model. We used the same feature set that has been used in the classification models and trained a Cox proportional hazards model [20]. Training and testing dataset are the same as the dataset used in the classification models. Model performance was evaluated by looking at the prediction accuracy on the testing dataset given the longest follow-up time of the testing dataset.

Cox proportional hazards model was trained with 5-fold cross-validation. However, the low accuracy score suggests under-fitting of the model during the training process. In order to include more data to better fit the model, we decided to have the model trained with the entire training dataset. Model performance will be discussed in the results section.

Chapter 4. RESULTS

1, Logistic Regression

	Prediction	
Truth	**0 (alive)**	**1 (dead)**
0 (alive)	11	9
1 (dead)	10	11

Table 4. Shows the performance of Logistic Regression model on the testing dataset. The overall accuracy rate is 53.66%.

2, Random Forest

	Prediction	
Truth	**0 (alive)**	**1(dead)**
0(alive)	10	10
1(dead)	7	14

Table 5. Confusion matrix for random forest model on the testing dataset. The overall accuracy rate is 58.54%.

3, Cox Proportional Hazards Model

	Prediction	
Truth	**0 (alive)**	**1(dead)**
0(alive)	9	11
1(dead)	10	11

Table 6. Confusion matrix for random forest model on the testing dataset. The overall accuracy rate is 48.78%.

Chapter 5. CONCLUSION AND FUTURE WORK

We engineered 676 features in total from the cellular location data. We used the K-S test to select 18 features from the 676 features at 95% significance level and used logistic regression and random forest models to predict 30-month survival probability. The model performance was tested on the randomly selected testing dataset and achieved an overall accuracy rate of 53.66% and 58.54%, respectively. We also tried Cox proportional hazards model and evaluated model performance with the same testing dataset as we have used for the logistic regression and random forest model. The accuracy rate for Cox proportional hazards model was 48.78%.

It is quite clear that none of logistic regression model, random forest model or Cox proportional hazards model is able to provide accurate prediction for survival outcome given that the best prediction accuracy score is 58.54% from the random forest model. One of the major challenges that limits us from achieving more accurate results and making further exploration is the small sample size. The whole data set been used in this study has only 101 observations. There is a high possibility that our current models were under-fitted. The small data size also prevents us from trying out more complicated models such as deep neural network and XGBoost.

Our collaborators previously found several cellular distribution patterns to be indicative of survival outcome using the same dataset [16]. They used Kaplan-Meier survival analysis coupled with log-rank test to determine if a certain feature is able to provide statistically significant prediction of long-term survival or short-term survival. This method has been previously discussed in the introduction section of this paper, which has several limitations including the lack of quantitative measurement about long-term and short-term survival time, etc. Some of the

features that have been found to be statistically significant predictors are: density of CD8+ cells in tumor region and stroma region (P-value = 0.01, 0.023), density of FoxP3+ cells in stroma region (P-value = 0.08), number of FoxP3+ cells within 30 μm of CD8+ cells in tumor region (P-value = 0.005) and number of PD-L1 + cells within 30 μm of CD8+ cells in stroma region (P-value < 0.0005).

Some of the features identified by the K-S test align with these findings. For example, we also found the distribution of the density of CD8+ cells in stroma region to be a statistically significant predictor in determining if a patient can survive 30 months (P-value = 0.0175, significant at 95% confidence level). However, none of our prediction models was able to provide accurate prediction based upon these features. We also hesitate to conclude that none of these features are strong indicators of survival because the small data size might underfit the model and thus fail to show clear signal.

We also note that the Kaplan-Meier survival analysis has been widely used in publications. Although this analysis is able to generate meaningful statistical insights on survival probability, researchers and clinicians have to be careful when interpreting results. For example, patients might be assigned to a long-term survival group with a significant P-value at a certain confidence level. This result, however, should not be simply interpreted as all the patients within such group having a higher probability of long-term survival compared with patients in other groups because, as our previous analysis and others have shown, certain patients in long-term survival group might have a shorter survival time than some of the patients in the short-term survival group.

During this project, we have established workflow and programmed code for feature engineering, data cleaning and modeling with multi-spectral tumor tissue image data. As our collaborators continue to collect more tumor tissue images and better data collection process to have high-quality data, we can apply similar analytical methods on the new data and update our findings. We will test our methods on the larger dataset and include more features such as demographical data and treatment data to have more concrete results. We will also expand our modeling exploration by predicting 1-year, 2-year or m-year survival probability instead of focusing on 3-year survival rate.

REFERENCE

1. Adams S, Gray RJ, Demaria S, Goldstein L, Perez EA, Shulman LN, et al. J OURNAL OF C LINICAL O NCOLOGY Prognostic Value of Tumor-Infiltrating Lymphocytes in Triple-Negative Breast Cancers From Two Phase III Randomized Adjuvant Breast Cancer Trials : ECOG 2197 and ECOG 1199. 2017;32(27).

2. Eerola A, Soini Y, Pääkkö P. A High Number of Tumor-infiltrating Lymphocytes Are Associated with a Small Tumor Size , Low Tumor Stage , and a Favorable Prognosis in Operated Small Cell Lung Carcinoma A High Number of Tumor-infiltrating Lymphocytes Are Associated with a Small Tumor Si. Clin Cancer Res. 2000;6(May):1875–81.

3. Kondratiev S, Sabo E, Yakirevich E, Lavie O, Resnick MB. Intratumoral CD8+ T lymphocytes as a prognostic factor of survival in endometrial carcinoma. Clin Cancer Res [Internet]. 2004;10(13):4450–6. Available from: http://www.ncbi.nlm.nih.gov/pubmed/15240536

4. Sharma P, Shen Y, Wen S, Yamada S, Jungbluth AA, Gnjatic S, et al. CD8 tumor-infiltrating lymphocytes are predictive of survival in muscle-invasive urothelial carcinoma. Proc Natl Acad Sci U S A [Internet]. 2007;104(10):3967–72. Available from: http://www.pubmedcentral.nih.gov/articlerender.fcgi?artid=1820692&tool=pmcentrez&rendertype=abstract

5. Obermeyer Z, Emanuel EJ. Predicting the Future — Big Data, Machine Learning, and Clinical Medicine. N Engl J Med [Internet]. 2016;375(13):1216–9. Available from: http://dx.doi.org/10.1056/NEJMp1606181

6. Siegel R, Naishadham D, Jemal A. Cancer Statistics , 2012. CA Cancer J Clin. 2012;62(1):10–29.

7. Sanderson RJ, Ironside JAD. Squamous cell carcinomas of the head and neck. BMJ. 2002;325(7368):822–7.

8. Egner JR. AJCC Cancer Staging Manual. Vol. 304, JAMA: The Journal of the American Medical Association. 2010. p. 1726.

9. Galon J, Pagès F, Marincola FM, Thurin M, Trinchieri G, Fox BA, et al. The immune score as a new possible approach for the classification of cancer. J Transl Med [Internet]. 2012;10(1):1. Available from:
http://translational-medicine.biomedcentral.com/articles/10.1186/1479-5876-10-1

10. Broussard EK, Mary L. Disis. TNM Staging in Colorectal Cancer: T Is for T Cell and M Is for Mem. J Clin Oncol. 2011;29(6):2011–3.

11. Mlecnik B, Bindea G, Pagès F, Galon J. Tumor immunosurveillance in human cancers. Cancer Metastasis Rev. 2011;30(1):5–12.

12. Curiel TJ, Coukos G, Zou L, Alvarez X, Cheng P, Mottram P, et al. Specific recruitment of regulatory T cells in ovarian carcinoma fosters immune privilege and predicts reduced survival. Nat Med. 2004;10(9):942–9.

13. Hiraoka N, Onozato K, Kosuge T, Hirohashi S. Prevalence of FOXP3+ regulatory T cells increases during the progression of pancreatic ductal adenocarcinoma and its premalignant lesions. Clin Cancer Res. 2006;12(18):5423–34.

14. Gao Q, Qiu SJ, Fan J, Zhou J, Wang XY, Xiao YS, et al. Intratumoral balance of regulatory and cytotoxic T cells is associated with prognosis of hepatocellular carcinoma after resection. J Clin Oncol. 2007;25(18):2586–93.

15. Goel MK, Khanna P, Kishore J. Understanding survival analysis: Kaplan-Meier estimate. Int J Ayurveda Res [Internet]. India: Medknow Publications & Media Pvt Ltd; 2010 Oct 8;1(4):274–8. Available from: http://www.ncbi.nlm.nih.gov/pmc/articles/PMC3059453/

16. Feng Z. Multiparametric Analysis of Tumor Immune Environment. 2016; Available from: http://digitalcommons.ohsu.edu/etd/3836/

17. Hornik K. Computing the Two-Sided Kolmogorov-Smirnov Distribution Richard. Journal of Statistical Software. J Stat Softw. 2009;31(2).

18. CARPENTER J. Bootstrap Methods and their Application. Eds. A. C. Davison and D. V. Hinkley. Cambridge University Press. 1997. Epidemiol Infect. Cambridge University Press; 1998;121(2):485–485.

19. Liaw A, Wiener M. Classification and Regression by randomForest. R News [Internet]. 2002;2(3):18–22. Available from: http://cran.r-project.org/doc/Rnews/

20. Terry M. Therneau, Patricia M. Grambsch. Modeling Survival Data: Extending the Cox Model. New York: Springer; 2000.

21. Tin Kam Ho. Random decision forests. Proc 3rd Int Conf Doc Anal Recognit [Internet]. 1995;1:278–82. Available from: http://ieeexplore.ieee.org/lpdocs/epic03/wrapper.htm?arnumber=598994

APPENDIX

Appendix 1. Patients Information

Gender (1 - male, 2 - female)	Status (0 - Alive, 1 - Dead)	Survival Time (Months)	Stage
1	0	65	1
1	0	16	1
2	0	17	2
2	1	6	4
2	0	8	4
2	0	17	2
2	0	18	4
1	0	60	2
2	1	11	2
1	0	15	4
2	1	28	2
1	1	25	1
2	0	61	3
1	0	60	3

1	1	6	4
1	0	34	1
1	0	60	4
1	0	60	3
1	0	65	1
2	0	65	1
1	0	59	4
1	0	65	1
1	1	18	4
1	1	23	4
1	0	30	2
1	0	60	1
1	1	17	4
2	0	65	3
1	0	60	4
1	0	6	4
1	1	17	2
1	1	11	2

2	0	41	3
1	1	3	4
1	1	7	4
1	0	17	4
1	1	13	2
1	1	15	4
1	1	28	4
2	1	22	2
2	0	28	4
1	1	6	4
1	1	6	4
1	0	65	2
2	1	13	4
1	1	7	4
1	1	23	4
1	1	44	4
2	0	54	1
1	0	26	2

1	1	8	4
1	1	10	4
1	0	65	4
1	0	65	2
1	1	51	1
2	0	48	2
1	0	65	2
1	1	20	4
1	0	65	1
1	0	49	4
1	0	38	4
1	1	8	4
1	1	8	3
1	1	4	4
2	1	42	1
1	1	8	4
1	1	59	4
1	0	65	2

2	0	56	4
1	1	6	4
1	1	23	4
1	1	20	4
1	0	48	1
1	0	42	1
1	0	57	2
2	0	30	4
1	0	37	2
1	0	39	3
1	0	50	1
2	1	25	4
1	0	3	4
1	0	57	4
1	1	26	4
1	0	58	3
1	1	9	4
2	0	65	4

1	1	18	4
1	0	35	3
2	1	13	3
2	1	6	4
2	1	18	4
1	1	7	4
1	0	48	3
2	1	4	4
2	1	26	4
1	0	36	1
1	1	14	4
1	0	35	4
1	0	35	4
1	0	26	4
2	0	48	2
1	1	27	3
1	1	3	4
1	1	15	4

1	0	33	2
1	1	11	3
1	0	21	2
1	0	33	4
1	1	16	4
1	1	17	4
2	1	16	4
1	1	21	4
1	0	65	2
1	0	32	4
1	0	31	3
2	0	26	1
1	0	30	4
1	1	16	2

Appendix 2. Feature List

1	mean_cd8_tumor	mean_foxp3_cd8_30_t	mean_tumor_tumor_100_s	mean_pdl1_cd4_100_s

2	mean_cd8_stroma	mean_tumor_macs_30	mean_tumor_tumor_100_t	mean_pdl1_cd4_100_t
3	mean_cd8_cd8_60	mean_tumor_macs_30_s	mean_cd8_r_cd4	mean_macs_cd4_30
4	mean_cd8_cd8_60_s	mean_tumor_macs_30_t	mean_cd8_r_cd4_tumor	mean_macs_cd4_30_s
5	mean_cd8_cd8_60_t	mean_tumor_macs_60	mean_cd8_r_cd4_stroma	mean_macs_cd4_30_t
6	mean_other_pdl1mac_60	mean_tumor_macs_60_s	mean_cd8_r_foxp3	mean_macs_cd4_60
7	mean_other_pdl1mac_60_s	mean_tumor_macs_60_t	mean_cd8_r_foxp3_tumor	mean_macs_cd4_60_s
8	mean_other_pdl1mac_60_t	mean_tumor_macs_100	mean_cd8_r_foxp3_stroma	mean_macs_cd4_60_t
9	mean_other_pdl1mac_100	mean_tumor_macs_100_s	mean_cd8_r_pdl1mac	mean_pdl1_tumor
10	mean_other_pdl1mac_100_s	mean_tumor_macs_100_t	mean_cd8_r_pdl1mac_tumor	mean_pdl1_stroma
11	mean_other_pdl1mac_100_t	mean_cd8_other_30	mean_cd8_r_pdl1mac_stroma	mean_macs_cd4_100
12	mean_tumor_pdl1mac_30	mean_cd8_other_30_s	mean_cd8_r_pdl1	mean_macs_cd4_100_s
13	mean_tumor_pdl1mac_30_s	mean_cd8_other_30_t	mean_cd8_r_pdl1_tumor	mean_macs_cd4_100_t
14	mean_tumor_pdl1mac_30_t	mean_cd8_other_60	mean_cd8_r_pdl1_stroma	mean_other_cd4_30

15	mean_tumor_pdl1mac_60	mean_cd8_other_60_s	mean_cd8_r_macs	mean_other_cd4_30_s
16	mean_tumor_pdl1mac_60_s	mean_cd8_other_60_t	mean_cd8_r_macs_tumor	mean_other_cd4_30_t
17	mean_tumor_pdl1mac_60_t	mean_cd8_other_100	mean_cd8_r_macs_stroma	mean_other_cd4_60
18	mean_tumor_pdl1mac_100	mean_cd8_other_100_s	mean_cd8_r_other	mean_other_cd4_60_s
19	mean_tumor_pdl1mac_100_s	mean_cd8_other_100_t	mean_cd8_r_other_tumor	mean_other_cd4_60_t
20	mean_tumor_pdl1mac_100_t	mean_cd4_other_30	mean_cd8_r_other_stroma	mean_other_cd4_100
21	mean_cd8_pdl1_30	mean_cd4_other_30_s	mean_cd8_r_tumor	mean_other_cd4_100_s
22	mean_cd8_pdl1_30_s	mean_cd4_other_30_t	mean_cd8_r_tumor_tumor	mean_other_cd4_100_t
23	mean_cd8_pdl1_30_t	mean_cd4_other_60	mean_cd8_r_tumor_stroma	mean_tumor_cd4_30
24	mean_cd8_pdl1_60	mean_cd4_other_60_s	mean_cd4_r_foxp3	mean_tumor_cd4_30_s
25	mean_cd8_pdl1_60_s	mean_cd4_other_60_t	mean_cd4_r_foxp3_tumor	mean_tumor_cd4_30_t
26	mean_cd8_pdl1_60_t	mean_cd4_other_100	mean_cd4_r_foxp3_stroma	mean_tumor_cd4_60
27	mean_cd8_pdl1_100	mean_cd4_other_100_s	mean_cd4_r_pdl1mac	mean_tumor_cd4_60_s
28	mean_cd8_pdl1_100_s	mean_cd4_other_100_t	mean_cd4_r_pdl1mac_tumor	mean_tumor_cd4_60_t

29	mean_cd8_pdl1_100_t	mean_foxp3_other_30	mean_cd4_r_pdl1mac_stroma	mean_tumor_cd4_100
30	mean_cd4_pdl1_30	mean_foxp3_other_30_s	mean_pdl1_cd8_30	mean_tumor_cd4_100_s
31	mean_cd4_pdl1_30_s	mean_foxp3_other_30_t	mean_pdl1_cd8_30_s	mean_tumor_cd4_100_t
32	mean_cd4_pdl1_30_t	mean_foxp3_cd8_60	mean_pdl1_cd8_30_t	mean_cd8_foxp3_30
33	mean_cd4_pdl1_60	mean_foxp3_cd8_60_s	mean_cd4_r_pdl1	mean_cd8_foxp3_30_s
34	mean_cd4_pdl1_60_s	mean_foxp3_cd8_60_t	mean_cd4_r_pdl1_tumor	mean_cd8_foxp3_30_t
35	mean_cd4_pdl1_60_t	mean_foxp3_other_60	mean_cd4_r_pdl1_stroma	mean_cd8_foxp3_60
36	mean_cd8_cd8_100	mean_foxp3_other_60_s	mean_cd4_r_macs	mean_cd8_foxp3_60_s
37	mean_cd8_cd8_100_s	mean_foxp3_other_60_t	mean_cd4_r_macs_tumor	mean_cd8_foxp3_60_t
38	mean_cd8_cd8_100_t	mean_foxp3_other_100	mean_cd4_r_macs_stroma	mean_cd8_foxp3_100
39	mean_cd4_pdl1_100	mean_foxp3_other_100_s	mean_cd4_r_other	mean_cd8_foxp3_100_s
40	mean_cd4_pdl1_100_s	mean_foxp3_other_100_t	mean_cd4_r_other_tumor	mean_cd8_foxp3_100_t
41	mean_cd4_pdl1_100_t	mean_pdl1mac_other_30	mean_cd4_r_other_stroma	mean_macs_tumor
42	mean_foxp3_pdl1_30	mean_pdl1mac_other_30_s	mean_cd4_r_tumor	mean_macs_stroma
43	mean_foxp3_pdl1_30_s	mean_pdl1mac_other_30_t	mean_cd4_r_tumor_tumor	mean_cd4_foxp3_30
44	mean_foxp3_pdl1_30_t	mean_pdl1mac_other_60	mean_cd4_r_tumor_stroma	mean_cd4_foxp3_30_s

45	mean_foxp3_pdl1_60	mean_pdl1mac_other_60_s	mean_foxp3_r_pdl1mac	mean_cd4_foxp3_30_t
46	mean_foxp3_pdl1_60_s	mean_pdl1mac_other_60_t	mean_foxp3_r_pdl1mac_tumor	mean_cd4_foxp3_60
47	mean_foxp3_pdl1_60_t	mean_pdl1mac_other_100	mean_foxp3_r_pdl1mac_stroma	mean_cd4_foxp3_60_s
48	mean_foxp3_pdl1_100	mean_pdl1mac_other_100_s	mean_foxp3_r_pdl1	mean_cd4_foxp3_60_t
49	mean_foxp3_pdl1_100_s	mean_pdl1mac_other_100_t	mean_foxp3_r_pdl1_tumor	mean_cd4_foxp3_100
50	mean_foxp3_pdl1_100_t	mean_pdl1_other_30	mean_foxp3_r_pdl1_stroma	mean_cd4_foxp3_100_s
51	mean_pdl1mac_pdl1_30	mean_pdl1_other_30_s	mean_foxp3_r_macs	mean_cd4_foxp3_100_t
52	mean_pdl1mac_pdl1_30_s	mean_pdl1_other_30_t	mean_foxp3_r_macs_tumor	mean_foxp3_foxp3_30
53	mean_pdl1mac_pdl1_30_t	mean_pdl1_other_60	mean_foxp3_r_macs_stroma	mean_foxp3_foxp3_30_s
54	mean_pdl1mac_pdl1_60	mean_pdl1_other_60_s	mean_foxp3_r_other	mean_foxp3_foxp3_30_t
55	mean_pdl1mac_pdl1_60_s	mean_pdl1_other_60_t	mean_foxp3_r_other_tumor	mean_foxp3_foxp3_60
56	mean_pdl1mac_pdl1_60_t	mean_pdl1_other_100	mean_foxp3_r_other_stroma	mean_foxp3_foxp3_60_s

57	mean_pdl1mac_pdl1_100	mean_pdl1_other_100_s	mean_foxp3_r_tumor	mean_foxp3_foxp3_60_t
58	mean_pdl1mac_pdl1_100_s	mean_pdl1_other_100_t	mean_foxp3_r_tumor_tumor	mean_foxp3_foxp3_100
59	mean_pdl1mac_pdl1_100_t	mean_macs_other_30	mean_foxp3_r_tumor_stroma	mean_foxp3_foxp3_100_s
60	mean_pdl1_pdl1_30	mean_macs_other_30_s	mean_pdl1mac_r_pdl1	mean_foxp3_foxp3_100_t
61	mean_pdl1_pdl1_30_s	mean_macs_other_30_t	mean_pdl1mac_r_pdl1_tumor	mean_pdl1mac_foxp3_30
62	mean_pdl1_pdl1_30_t	mean_macs_other_60	mean_pdl1mac_r_pdl1_stroma	mean_pdl1mac_foxp3_30_s
63	mean_pdl1_pdl1_60	mean_macs_other_60_s	mean_pdl1_cd8_60	mean_pdl1mac_foxp3_30_t
64	mean_pdl1_pdl1_60_s	mean_macs_other_60_t	mean_pdl1_cd8_60_s	mean_pdl1mac_foxp3_60
65	mean_pdl1_pdl1_60_t	mean_foxp3_cd8_100	mean_pdl1_cd8_60_t	mean_pdl1mac_foxp3_60_s
66	mean_pdl1_pdl1_100	mean_foxp3_cd8_100_s	mean_pdl1mac_r_macs	mean_pdl1mac_foxp3_60_t
67	mean_pdl1_pdl1_100_s	mean_foxp3_cd8_100_t	mean_pdl1mac_r_macs_tumor	mean_pdl1mac_foxp3_100
68	mean_pdl1_pdl1_100_t	mean_macs_other_100	mean_pdl1mac_r_macs_stroma	mean_pdl1mac_foxp3_100_s
69	mean_cd4_cd8_30	mean_macs_other_100_	mean_pdl1mac_r_other	mean_pdl1mac_foxp3_100

		s		_t
70	mean_cd4_cd8_30_s	mean_macs_other_100_t	mean_pdl1mac_r_other_tumor	mean_pdl1_foxp3_30
71	mean_cd4_cd8_30_t	mean_other_other_30	mean_pdl1mac_r_other_stroma	mean_pdl1_foxp3_30_s
72	mean_macs_pdl1_30	mean_other_other_30_s	mean_pdl1mac_r_tumor	mean_pdl1_foxp3_30_t
73	mean_macs_pdl1_30_s	mean_other_other_30_t	mean_pdl1mac_r_tumor_tumor	mean_other_tumor
74	mean_macs_pdl1_30_t	mean_other_other_60	mean_pdl1mac_r_tumor_stroma	mean_other_stroma
75	mean_macs_pdl1_60	mean_other_other_60_s	mean_pdl1_r_macs	mean_pdl1_foxp3_60
76	mean_macs_pdl1_60_s	mean_other_other_60_t	mean_pdl1_r_macs_tumor	mean_pdl1_foxp3_60_s
77	mean_macs_pdl1_60_t	mean_other_other_100	mean_pdl1_r_macs_stroma	mean_pdl1_foxp3_60_t
78	mean_macs_pdl1_100	mean_other_other_100_s	mean_pdl1_r_other	mean_pdl1_foxp3_100
79	mean_macs_pdl1_100_s	mean_other_other_100_t	mean_pdl1_r_other_tumor	mean_pdl1_foxp3_100_s
80	mean_macs_pdl1_100_t	mean_tumor_other_30	mean_pdl1_r_other_stroma	mean_pdl1_foxp3_100_t
81	mean_other_pdl1_30	mean_tumor_other_30_s	mean_pdl1_r_tumor	mean_macs_foxp3_30

82	mean_other_pdl1_30_s	mean_tumor_other_30_t	mean_pdl1_r_tumor_tumor	mean_macs_foxp3_30_s
83	mean_other_pdl1_30_t	mean_tumor_other_60	mean_pdl1_r_tumor_stroma	mean_macs_foxp3_30_t
84	mean_other_pdl1_60	mean_tumor_other_60_s	mean_macs_r_other	mean_macs_foxp3_60
85	mean_other_pdl1_60_s	mean_tumor_other_60_t	mean_macs_r_other_tumor	mean_macs_foxp3_60_s
86	mean_other_pdl1_60_t	mean_tumor_other_100	mean_macs_r_other_stroma	mean_macs_foxp3_60_t
87	mean_other_pdl1_100	mean_tumor_other_100_s	mean_macs_r_tumor	mean_macs_foxp3_100
88	mean_other_pdl1_100_s	mean_tumor_other_100_t	mean_macs_r_tumor_tumor	mean_macs_foxp3_100_s
89	mean_other_pdl1_100_t	mean_cd8_tumor_30	mean_macs_r_tumor_stroma	mean_macs_foxp3_100_t
90	mean_tumor_pdl1_30	mean_cd8_tumor_30_s	mean_other_r_tumor	mean_other_foxp3_30
91	mean_tumor_pdl1_30_s	mean_cd8_tumor_30_t	mean_other_r_tumor_tumor	mean_other_foxp3_30_s
92	mean_tumor_pdl1_30_t	mean_cd8_tumor_60	mean_other_r_tumor_stroma	mean_other_foxp3_30_t
93	mean_tumor_pdl1_60	mean_cd8_tumor_60_s	mean_pdl1_cd8_100	mean_other_foxp3_60
94	mean_tumor_pdl1_60	mean_cd8_tumor_60_t	mean_pdl1_cd8_100_s	mean_other_foxp3_60_s

	_s			
95	mean_tumor_pdl1_60_t	mean_cd8_tumor_100	mean_pdl1_cd8_100_t	mean_other_foxp3_60_t
96	mean_tumor_pdl1_100	mean_cd8_tumor_100_s	mean_macs_cd8_30	mean_other_foxp3_100
97	mean_tumor_pdl1_100_s	mean_cd8_tumor_100_t	mean_macs_cd8_30_s	mean_other_foxp3_100_s
98	mean_tumor_pdl1_100_t	mean_pdl1mac_cd8_30	mean_macs_cd8_30_t	mean_other_foxp3_100_t
99	mean_cd8_macs_30	mean_pdl1mac_cd8_30_s	mean_macs_cd8_60	mean_tumor_foxp3_30
100	mean_cd8_macs_30_s	mean_pdl1mac_cd8_30_t	mean_macs_cd8_60_s	mean_tumor_foxp3_30_s
101	mean_cd8_macs_30_t	mean_cd4_tumor_30	mean_macs_cd8_60_t	mean_tumor_foxp3_30_t
102	mean_cd4_cd8_60	mean_cd4_tumor_30_s	mean_macs_cd8_100	mean_tumor_foxp3_60
103	mean_cd4_cd8_60_s	mean_cd4_tumor_30_t	mean_macs_cd8_100_s	mean_tumor_foxp3_60_s
104	mean_cd4_cd8_60_t	mean_cd4_tumor_60	mean_macs_cd8_100_t	mean_tumor_foxp3_60_t
105	mean_cd8_macs_60	mean_cd4_tumor_60_s	mean_other_cd8_30	mean_tumor_tumor
106	mean_cd8_macs_60_s	mean_cd4_tumor_60_t	mean_other_cd8_30_s	mean_tumor_stroma
107	mean_cd8_macs_60_t	mean_cd4_tumor_100	mean_other_cd8_30_t	mean_tumor_foxp3_100
108	mean_cd8_macs_100	mean_cd4_tumor_100_s	mean_other_cd8_60	mean_tumor_foxp3_100_s
109	mean_cd8_macs_100_s	mean_cd4_tumor_100_t	mean_other_cd8_60_s	mean_tumor_foxp3_100_t

110	mean_cd8_macs_100_t	mean_foxp3_tumor_30	mean_other_cd8_60_t	mean_cd8_pdl1mac_30
111	mean_cd4_macs_30	mean_foxp3_tumor_30_s	mean_other_cd8_100	mean_cd8_pdl1mac_30_s
112	mean_cd4_macs_30_s	mean_foxp3_tumor_30_t	mean_other_cd8_100_s	mean_cd8_pdl1mac_30_t
113	mean_cd4_macs_30_t	mean_foxp3_tumor_60	mean_other_cd8_100_t	mean_cd8_pdl1mac_60
114	mean_cd4_macs_60	mean_foxp3_tumor_60_s	mean_foxp3_tumor	mean_cd8_pdl1mac_60_s
115	mean_cd4_macs_60_s	mean_foxp3_tumor_60_t	mean_foxp3_stroma	mean_cd8_pdl1mac_60_t
116	mean_cd4_macs_60_t	mean_foxp3_tumor_100	mean_tumor_cd8_30	mean_cd8_pdl1mac_100
117	mean_cd4_macs_100	mean_foxp3_tumor_100_s	mean_tumor_cd8_30_s	mean_cd8_pdl1mac_100_s
118	mean_cd4_macs_100_s	mean_foxp3_tumor_100_t	mean_tumor_cd8_30_t	mean_cd8_pdl1mac_100_t
119	mean_cd4_macs_100_t	mean_pdl1mac_tumor_30	mean_tumor_cd8_60	mean_cd4_pdl1mac_30
120	mean_foxp3_macs_30	mean_pdl1mac_tumor_30_s	mean_tumor_cd8_60_s	mean_cd4_pdl1mac_30_s
121	mean_foxp3_macs_30_s	mean_pdl1mac_tumor_30_t	mean_tumor_cd8_60_t	mean_cd4_pdl1mac_30_t
122	mean_foxp3_macs_30	mean_pdl1mac_tumor_	mean_tumor_cd8_100	mean_cd4_pdl1mac_60

	_t	60		
123	mean_foxp3_macs_60	mean_pdl1mac_tumor_60_s	mean_tumor_cd8_100_s	mean_cd4_pdl1mac_60_s
124	mean_foxp3_macs_60_s	mean_pdl1mac_tumor_60_t	mean_tumor_cd8_100_t	mean_cd4_pdl1mac_60_t
125	mean_foxp3_macs_60_t	mean_pdl1mac_tumor_100	mean_cd8_cd4_30	mean_cd4_pdl1mac_100
126	mean_foxp3_macs_100	mean_pdl1mac_tumor_100_s	mean_cd8_cd4_30_s	mean_cd4_pdl1mac_100_s
127	mean_foxp3_macs_100_s	mean_pdl1mac_tumor_100_t	mean_cd8_cd4_30_t	mean_cd4_pdl1mac_100_t
128	mean_foxp3_macs_100_t	mean_pdl1_tumor_30	mean_cd8_cd4_60	mean_foxp3_pdl1mac_30
129	mean_pdl1mac_macs_30	mean_pdl1_tumor_30_s	mean_cd8_cd4_60_s	mean_foxp3_pdl1mac_30_s
130	mean_pdl1mac_macs_30_s	mean_pdl1_tumor_30_t	mean_cd8_cd4_60_t	mean_foxp3_pdl1mac_30_t
131	mean_pdl1mac_macs_30_t	mean_pdl1mac_cd8_60	mean_cd8_cd4_100	mean_foxp3_pdl1mac_60
132	mean_pdl1mac_macs_60	mean_pdl1mac_cd8_60_s	mean_cd8_cd4_100_s	mean_foxp3_pdl1mac_60_s
133	mean_pdl1mac_macs_60_s	mean_pdl1mac_cd8_60_t	mean_cd8_cd4_100_t	mean_foxp3_pdl1mac_60_t

134	mean_pdl1mac_macs_60_t	mean_pdl1_tumor_60	mean_cd4_cd4_30	mean_foxp3_pdl1mac_100
135	mean_cd4_cd8_100	mean_pdl1_tumor_60_s	mean_cd4_cd4_30_s	mean_foxp3_pdl1mac_100_s
136	mean_cd4_cd8_100_s	mean_pdl1_tumor_60_t	mean_cd4_cd4_30_t	mean_foxp3_pdl1mac_100_t
137	mean_cd4_cd8_100_t	mean_pdl1_tumor_100	mean_cd4_cd4_60	mean_cd8_cd8_30
138	mean_pdl1mac_macs_100	mean_pdl1_tumor_100_s	mean_cd4_cd4_60_s	mean_cd8_cd8_30_s
139	mean_pdl1mac_macs_100_s	mean_pdl1_tumor_100_t	mean_cd4_cd4_60_t	mean_cd8_cd8_30_t
140	mean_pdl1mac_macs_100_t	mean_macs_tumor_30	mean_cd4_cd4_100	mean_pdl1mac_pdl1mac_30
141	mean_pdl1_macs_30	mean_macs_tumor_30_s	mean_cd4_cd4_100_s	mean_pdl1mac_pdl1mac_30_s
142	mean_pdl1_macs_30_s	mean_macs_tumor_30_t	mean_cd4_cd4_100_t	mean_pdl1mac_pdl1mac_30_t
143	mean_pdl1_macs_30_t	mean_macs_tumor_60	mean_foxp3_cd4_30	mean_pdl1mac_pdl1mac_60
144	mean_pdl1_macs_60	mean_macs_tumor_60_s	mean_foxp3_cd4_30_s	mean_pdl1mac_pdl1mac_60_s
145	mean_pdl1_macs_60_s	mean_macs_tumor_60_t	mean_foxp3_cd4_30_t	mean_pdl1mac_pdl1mac_60_t

146	mean_pdl1_macs_60_t	mean_macs_tumor_100	mean_pdl1mac_tumor	mean_pdl1mac_pdl1mac_100
147	mean_pdl1_macs_100	mean_macs_tumor_100_s	mean_pdl1mac_stroma	mean_pdl1mac_pdl1mac_100_s
148	mean_pdl1_macs_100_s	mean_macs_tumor_100_t	mean_foxp3_cd4_60	mean_pdl1mac_pdl1mac_100_t
149	mean_pdl1_macs_100_t	mean_other_tumor_30	mean_foxp3_cd4_60_s	mean_pdl1_pdl1mac_30
150	mean_macs_macs_30	mean_other_tumor_30_s	mean_foxp3_cd4_60_t	mean_pdl1_pdl1mac_30_s
151	mean_macs_macs_30_s	mean_other_tumor_30_t	mean_foxp3_cd4_100	mean_pdl1_pdl1mac_30_t
152	mean_macs_macs_30_t	mean_other_tumor_60	mean_foxp3_cd4_100_s	mean_pdl1_pdl1mac_60
153	mean_macs_macs_60	mean_other_tumor_60_s	mean_foxp3_cd4_100_t	mean_pdl1_pdl1mac_60_s
154	mean_macs_macs_60_s	mean_other_tumor_60_t	mean_pdl1mac_cd4_30	mean_pdl1_pdl1mac_60_t
155	mean_macs_macs_60_t	mean_other_tumor_100	mean_pdl1mac_cd4_30_s	mean_pdl1_pdl1mac_100
156	mean_macs_macs_100	mean_other_tumor_100_s	mean_pdl1mac_cd4_30_t	mean_pdl1_pdl1mac_100_s
157	mean_macs_macs_100_s	mean_other_tumor_100_t	mean_pdl1mac_cd4_60	mean_pdl1_pdl1mac_100_t

158	mean_macs_macs_100_t	mean_tumor_tumor_30	mean_pdl1mac_cd4_60_s	mean_macs_pdl1mac_30
159	mean_other_macs_30	mean_tumor_tumor_30_s	mean_pdl1mac_cd4_60_t	mean_macs_pdl1mac_30_s
160	mean_other_macs_30_s	mean_tumor_tumor_30_t	mean_pdl1mac_cd4_100	mean_macs_pdl1mac_30_t
161	mean_other_macs_30_t	mean_tumor_tumor_60	mean_pdl1mac_cd4_100_s	mean_macs_pdl1mac_60
162	mean_other_macs_60	mean_tumor_tumor_60_s	mean_pdl1mac_cd4_100_t	mean_macs_pdl1mac_60_s
163	mean_other_macs_60_s	mean_tumor_tumor_60_t	mean_pdl1_cd4_30	mean_macs_pdl1mac_60_t
164	mean_other_macs_60_t	mean_cd4_tumor	mean_pdl1_cd4_30_s	mean_macs_pdl1mac_100
165	mean_other_macs_100	mean_cd4_stroma	mean_pdl1_cd4_30_t	mean_macs_pdl1mac_100_s
166	mean_other_macs_100_s	mean_pdl1mac_cd8_100	mean_pdl1_cd4_60	mean_macs_pdl1mac_100_t
167	mean_other_macs_100_t	mean_pdl1mac_cd8_100_s	mean_pdl1_cd4_60_s	mean_other_pdl1mac_30
168	mean_foxp3_cd8_30	mean_pdl1mac_cd8_100_t	mean_pdl1_cd4_60_t	mean_other_pdl1mac_30_s
169	mean_foxp3_cd8_30_s	mean_tumor_tumor_100	mean_pdl1_cd4_100	mean_other_pdl1mac_30_t